ADVANCED OPEN-CYCLE DESICCANT COOLING SYSTEM

Y. J. Ko, D. Charoensupaya and Z. Lavan
Illinois Institute of Technology
Department of Mechanical and Aerospace Engineering
10 West Thirty-Second Street, Chicago, Illinois 60616

ABSTRACT

The concept of staged regeneration as means of improving the desiccant cooling system performance is the subject of investigation in this study. In the staged regeneration, the regeneration section of desiccant dehumidifier is divided into two parts and only the latter fraction is subjected to the desorption air stream which has been heated to the desired regeneration temperature.

In the present work, the mathematical model describing the heat and mass transfer processes that occur during sorption of moisture in the desiccant dehumidifier includes both the gas-side (film) and solid-side resistances for heat and mass transports. The moisture diffusion in the desiccant material is expressed by gas-phase diffusion and surface diffusion. Effects of several parameters on the performance of desiccant cooling system with staged regeneration are investigated and the results of present model are compared with those of the lumped-resistance model.

Results of this study show that coefficient of performance of the desiccant cooling system can be substantially improved by using the staged regeneration concept. There is an optimum stage fraction and optimum cycle time for given system parameters and operating conditions. The results also indicate that the cooling system performance is higher than that predicted by the lumped-resistance model.

NOMENCLATURE

a_d	thickness of desiccant, m
a_p	height of process stream channel, m
a_w	thickness of supporting wall, m
A	mass transfer area, m^2
Bi_h	heat transfer Biot number
Bi_m	mass transfer Biot number defined by Equation (16)
Bi_{mo}	overall mass transfer Biot number defined by Equation (20)
C_a	specific heat of dry air, kJ/kg air °C
C_d	specific heat of desiccant, kJ/kg desiccant °C
C_w	specific heat of supporting wall, kJ/kg °C
COP	thermal coefficient of performance
D_G	effective gas-phase diffusivity, m^2/s
D_S	effective surface diffusivity, m^2/s
h_{fg}	latent heat of vaporization of water, kJ/kg H_2O
h_p	heat transfer coefficient, kW/m^2 °C
H_a	enthalpy of gas-phase in desiccant, kJ/kg air
H_p	enthalpy of process stram air, kJ/kg air
k_d	apparent thermal conductivity of desiccant, kW/m °C
K_y	mass transfer coefficient of process stream, kg/m^2 s
m_p	mass flowrate of process stream air, kg/s
NTU	number of transfer unit
NTU_{fm}	mass transfer NTU based on film resistance defined by Equation (22)
NTU_{om}	overall mass transfer NTU defined by Equation (18)
Q	heat of sorption, kJ/kg H_2O
r	isotherm shape factor
RH	relative humidity
SF	stage fraction
t	time, s
T	temperature, °C
T_d	desiccant temperature, °C
T_{do}	initial desiccant temperature, °C
T_p	temperature of process stream air, °C
T_{pi}	inlet temperature of process stream air, °C
T_w	wall temperature, °C
U_m	overall mass transfer coefficient, kJ/m^2 s
W_d	moisture content in desiccant, kg H_2O/kg desiccant
W_{max}	maximum loading of desiccant, kg H_2O/kg desiccant
x	space variable in the flow direction, m
x_t	channel length, m
X	nondimensional space variable defined by Equation (14)
X_f	nondimensional channel length
y	space variable in channel width direction, m
y_t	channel width, m
Y	humidity ratio, kg H_2O/kg dry air
Y_d	humidity ratio in the gas-phase of desiccant, kg H_2O/kg dry air
Y_{do}	initial humidity ratio in the gas-phase of desiccant, kg H_2O/kg dry air
Y_p	humidity ratio of process stream air, kg H_2O/kg dry air
Y_{pi}	inlet humidity ratio of process stream air, kg H_2O/kg dry air
z	space variable in channel height direction, m
Z	nondimensional space variable defined by Equation (15)
ε_d	porosity of desiccant
ρ_a	air density, kg air/m^3
ρ_d	true density of desiccant, kg desiccant/m^3
ρ_w	density of supporting wall, kg/m^3
τ	nondimensional time defined by Equation (13)
τ_f	nondimensional sorption time

Proceedings of the Sixth Symposium on Improving Building Systems in Hot and Humid Climates, Dallas, TX, October 3-4, 1989

INTRODUCTION

An extension of desiccant dehumidification to cooling system was done in an early development by Pennington (1). Dunkle (2) introduced a method of solar air-conditioning using an open-cycle desiccant system. Earlier researchers (3, 4) investigated the system with adiabatic dehumidifier operating with equal adsorption and desorption period..

Huske et al (5) and Collier and Cohen (6) showed that the system performance can be improved by adding inert material to increase the heat capacity of the desiccant matrices. Worek and Lavan (7) and Mathiprakasam (8) studied the desiccant cooling system using cross-cooled dehumidifiers where the heat of sorption is removed by cooling air stream. The results indicated that the cooling capacity of the system is improved, since the desiccant is at lower temperature during adsorption process and therefore has higher sorption capacity.

In 1966, Glav (9) introduced a technique called staged regeneration for the rotary type air-conditioning apparatus. In this concept, the regeneration section of desiccant dehumidifier is divided into two parts and only the latter fraction is subjected to the desorption air stream which has been heated to the desired regeneration temperature.

The dynamic sorption analysis for the desiccant dehumidifier is important for the proper design of desiccant cooling system. Banks et al (10) introduced a linearized solutions using analogy method for the adiabatic dehumidifier. Roy and Gidaspow (11) used Green's function to get the nonlinear solution for the cross-cooled dehumidifier. A solution was also obtained by Mathiprakasam and Lavan (12) using Laplace Transforms.

Many investigators (13, 14, 15, 16) used lumped-resistance models to describe the heat and mass transports occur during the sorption processes in the dehumidifier. These models do not include the solid-side resistances, and if necessary the solid-side resistances will be compensated by artificially increasing of film resistances.

In the present work, both film and solid-side resistances to heat and mass transports are considered to analyze the dynamic sorption in the dehimidifier, and the staged regeneration concept as means to improve the system performance is investigated. The effects of solid-side mass transfer resistance are also investigated and are compared to those obtained by the lumped-resistance model (13).

COOLING SYSTEM CONFIGURATION

Various cooling systems utilizing solid desiccants are discussed in (3). In this study, adiabatic dehumidifier desiccant cooling systems operating in the ventilation mode are considered.

Figure 1 shows the schematic diagram of the system and the corresponding psychrometric diagram is shown in Figure 2. In this system, the process air stream for the adsorption process is drawn from outside and is passed through the dehumidifier. The warm dry air leaving the dehumidifier enters the heat exchanger where it is sensibly cooled down to near room temperature. This air stream is then passed through an evaporative cooler where it is cooled and humidified before entering the conditioned room. During the desorption process, air is drawn from the conditioned room, humidified and cooled in an evaporative cooler and enters the heat exchanger in which it recovers the sensible heat from the adsorption air stream. This warm air stream is then heated to the desired regeneration temperature by a heat source, is passed through the dehumidifier to regenerate the desiccant material and is discarded to the outside.

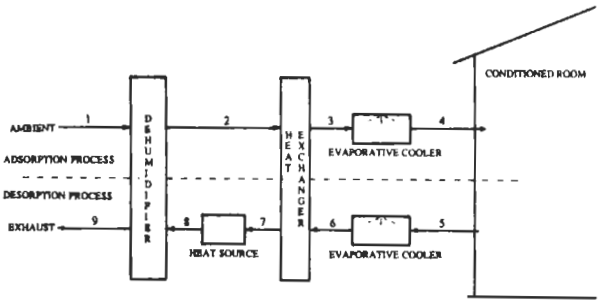

Figure 1. Schematic diagram of desiccant cooling system without staged regeneration

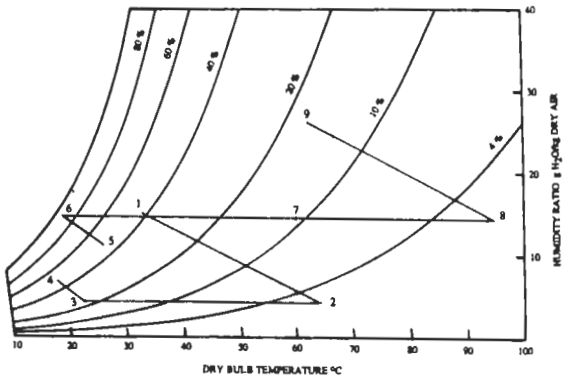

Figure 2. Psychrometric diagram of desiccant cooling system without staged regeneration

Figures 3 and 4 show the schematic and the corresponding psychrometric diagram of an adiabatic dehumidifier cooling system in the ventilation mode with staged regeneration. The adsorption process is the same as of the conventional cooling system shown in Figure 1. For the desorption process, a fraction of air stream enters the dehumidifier without passing through the heat source for the initial period and the latter fraction is heated to the regeneration temperature. The stage fraction (SF) is defined as the ratio of mass flow of process air stream through the heat source to the total mass flow during the desorption process. Since the mass flowrates and duration of the adsorption and desorption

processes are equal, the stage fraction can be defined by the process time fraction. Stage fraction equals to unity means that all the desorption air stream passes through the heat source, i.e. no staged regeneration.

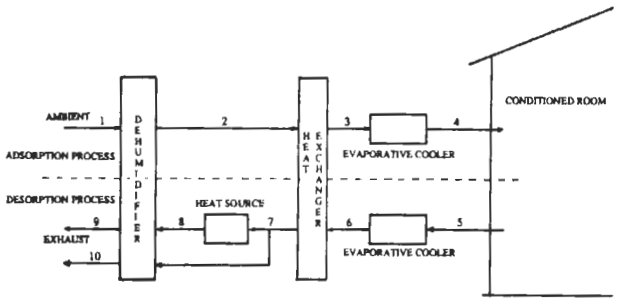

Figure 3. Schematic diagram of desiccant cooling system with staged regeneration

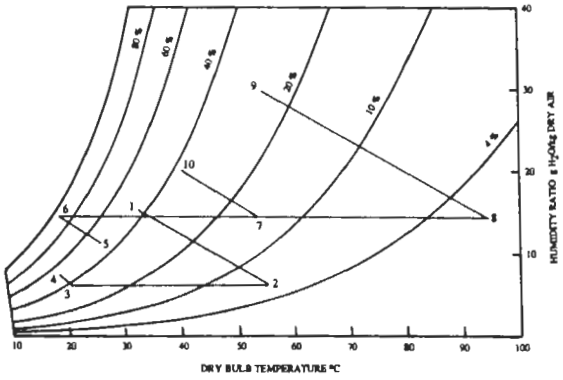

Figure 4. Psychrometric diagram of desiccant cooling system with staged regeneration

MATHEMATICAL MODEL

The analysis of sorption processes in the desiccant dehumidifier requires a detailed description of the diffusion phenomena in porous desiccant materials which can be considered as a multi-phase system consisting of solid desiccant, sorbate and inert gas (air). Figure 5 shows the physical model for moisture transfer in the pores. When water molecules enter desiccant pores, some molecules will be attached to the surface of the pore, while others diffuse into the pore by gas-phase diffusion which can be either an ordinary diffusion or Knudsen diffusion depending on the pore diameter. The water molecules which have been attached to the pore surface then can diffuse into the pore along the wall of the pore and is called surface diffusion.

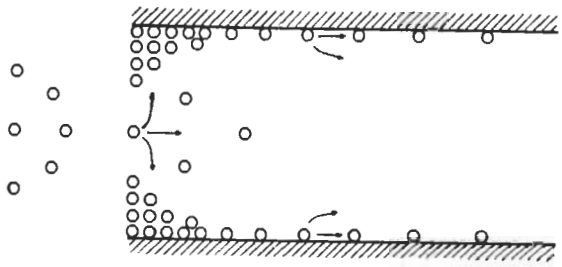

Figure 5. Physical model of mass transfer in desiccant pore

Figure 6 shows an element of a desiccant dehumidifier. The governing equations for mass and heat transfer can be described with the following assumptions :

1. The mass and heat diffusions in the channels are small compared to the convective transfer, thus can be neglected.
2. The temperature and concentration gradients across the channel are negligible.
3. The mass and heat transfer rates between the streams and the solid desiccant material surface can be calculated from Nusselt and Sherwood numbers which are constant.
4. The nonhygroscopic supporting material is considered to be a good conducting material and the thermal contact resistance between supporting wall and the desiccant material can be neglected. Therefore its temperature is the same as the contacting desiccant material and is uniform in y and z directions.
5. The mass and thermal diffusions in the y and z directions are neglected in the solid desiccant material.
6. Equilibrium always exists between the sorbate in the gas phase and the sorbent.

Using these assumptions, the governing equations describing the heat and mass transports in the dehumidifier can be derived (17) and are given as follows:

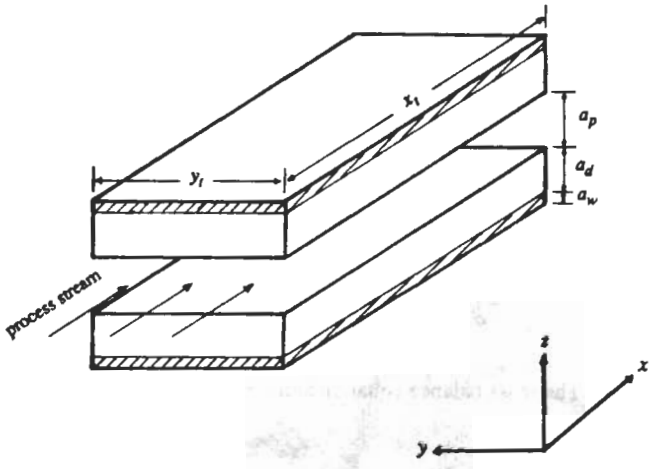

Figure 6. Schematic of desiccant dehumidifier element

The mass diffusion equation with the initial and boundary conditions,

$$[\varepsilon_d + (1-\varepsilon_d)\frac{\rho_d}{\rho_a}\frac{\partial W_d}{\partial Y_d}]\frac{\partial Y_d}{\partial t} - (D_G + D_s\frac{\rho_d}{\rho_a}\frac{\partial W_d}{\partial Y_d})\frac{\partial^2 Y_d}{\partial z^2}$$

$$= D_s\frac{\rho_d}{\rho_a}\frac{\partial W_d}{\partial T_d}\frac{\partial^2 T_d}{\partial z^2} - (1-\varepsilon_d)\frac{\rho_d}{\rho_a}\frac{\partial W_d}{\partial T_d}\frac{\partial T_d}{\partial t} \quad (1)$$

$$Y_d(0, x, z) = Y_{d\,0}(x, z) \quad (2)$$

$$(D_G + D_s\frac{\rho_d}{\rho_a}\frac{\partial W_d}{\partial Y_d})\frac{\partial Y_d(t, x, 0)}{\partial z}$$

$$+ D_s\frac{\rho_d}{\rho_a}\frac{\partial W_d}{\partial T_d}\frac{\partial T_d(t, x, 0)}{\partial z} = 0 \quad (3)$$

$$(\rho_a D_G + \rho_d D_s\frac{\partial W_d}{\partial Y_d})\frac{\partial Y_d(t, x, a_d)}{\partial z}$$

$$+ \rho_d D_s\frac{\partial W_d}{\partial T_d}\frac{\partial T_d(t, x, a_d)}{\partial z} = K_y[Y_p(t, x) - Y_d(t, x, a_d)] \quad (4)$$

Thermal diffusion equation with the initial and boundary conditions,

$$(\frac{\varepsilon_d}{1-\varepsilon_d}\frac{\rho_a}{\rho_d}\frac{\partial H_a}{\partial T_d} + C_d - Q\frac{\partial W_d}{\partial T_d})\frac{\partial T_d}{\partial t} - \frac{k_d}{(1-\varepsilon_d)\rho_d}\frac{\partial^2 T_d}{\partial z^2}$$

$$= (Q\frac{\partial W_d}{\partial Y_d} - \frac{\varepsilon_d}{1-\varepsilon_d}\frac{\rho_a}{\rho_d}\frac{\partial H_a}{\partial Y_d})\frac{\partial Y_d}{\partial t} \quad (5)$$

$$T_d(0, x, z) = T_{d\,0}(x, z) \quad (6)$$

$$k_d\frac{\partial T_d(t, x, 0)}{\partial z} = \rho_w a_w C_w\frac{\partial T_w(t, x)}{\partial t}$$

$$+ h_c[T_d(t, x) - T_c(t, x)] \quad (7)$$

$$- k_d\frac{\partial T_d(t, x, a_d)}{\partial z} = h_p[T_d(t, x, a_d) - T_p(t, x)] \quad (8)$$

The mass balance equation and the inlet condition for process stream,

$$\frac{\dot{m}_p}{2K_y y_t}\frac{\partial Y_p}{\partial x} = Y_d(t, x, a_d) - Y_p(t, x) \quad (9)$$

$$Y_p(t, 0) = Y_{pi}(t) \quad (10)$$

The heat balance equation and the inlet condition for process stream,

$$\frac{\dot{m}_p}{2h_p y_t}\frac{\partial H_p}{\partial T_p}\frac{\partial T_p}{\partial x} = -[T_p(t, x) - T_d(t, x, a_d)] \quad (11)$$

$$T_p(t, 0) = T_{pi}(t) \quad (12)$$

The governing Equations (1), (5) and (11) are nonlinear and coupled. These equations are rearranged using the following nondimensional independant variables:

$$\tau = \frac{D_G t}{a_d^2} \quad (13)$$

$$X = \frac{2K_y y_t x}{\dot{m}_p} \quad (14)$$

$$Z = \frac{z}{a_d} \quad (15)$$

A finite difference technique is used with backward differences for time and central differences for space for the mass and thermal diffusion Equations (1) and (5) in the desiccant material. For Equations (9) and (11), a forward difference scheme is used.

RESULTS AND DISSUSIONS

Numerical solutions to the governing equations were obtained using the operating conditions listed in Table 1. All of the results are presented for the cooling system and dehumidifier under periodic steady-state which is indicated by identical performance of successive cycles.

The cooling system performance is characterized by the thermal coefficient of performance (COP) and the cooling capacity. The thermal coefficient of performance is defined as the ratio of the cooling capacity to the thermal energy input. The cooling capacity of the system is defined as the enthalpy difference of the process air stream between the inlet and outlet of the conditioned space. Since adiabatic humidification evaporative coolers are used, the cooling capacity can be calculated from the evaporative cooler inlet conditions of the adsorption process and the evaporative cooler outlet conditions of the desorption process. The thermal energy input is calculated from the enthalpy difference of the desorption air stream across the heat source.

Table 1. Summary of system operation conditions

Dehumidifier operation mode	adiabatic
Process stream cycle	ventilation
Ambient temperature	35°C
Ambient humidity ratio	0.0142 kg H_2O/kg air
Regeneration temperature	95°C
Heat exchanger effectiveness	0.93
Evaporative cooler effectiveness	0.95
Conditioned room temperature	26.7°C
Conditioned room humidity ratio	0.0111 kg H_2O/kg air
Equilibrium relation*	r = 0.1
Maximum loading	0.4 kg H_2O/kg desiccant
Heat of sorption	h_{fg}

* Equilibrium relation:

$$\frac{W}{W_{max}} = \frac{RH}{r + (1 - r)RH}$$

Effect of Stage Fraction on the Performance

Figures 7 and 8 show the effect of nondimensional cycle time on the COP and the cooling capacity for various stage fraction. There is an optimum cycle time for a given stage fraction. However, there is a only a small difference in the system performance from the optimum cycle time.

The optimum COP with corresponding cooling capacity are shown as function of stage fraction in Figures 9 and 10 respectively. The COP increases with increasing SF up to SF=0.3 ~ 0.4 which is the optimum SF, then it decreases. But the cooling capacity continuously increases with increasing SF. The increasing rate of cooling capacity is large at small SF and it

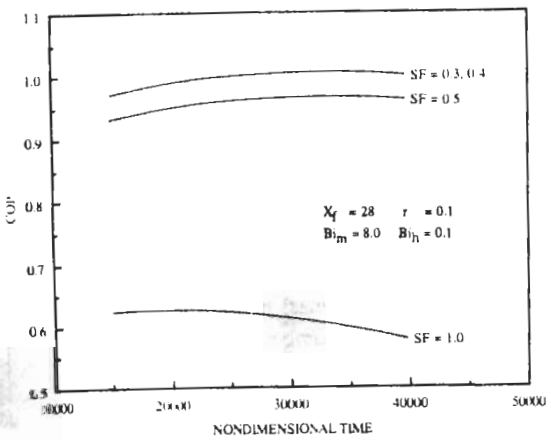

Figure 7. Effect of nondimensional cycle time on *COP* with variable stage fraction

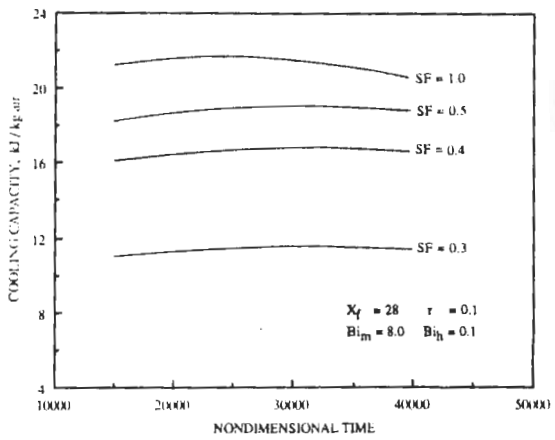

Figure 8. Effect of nondimensional cycle time on cooling capacity with variable stage fraction

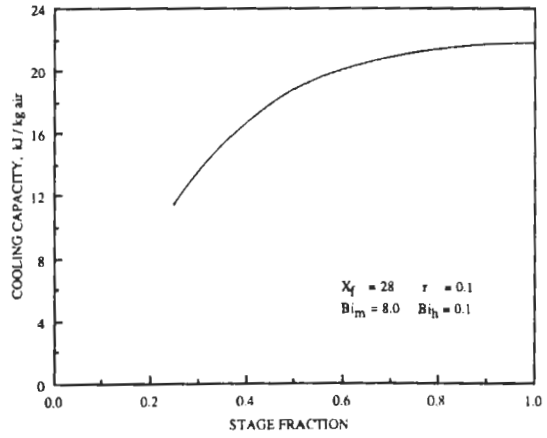

Figure 9. Effect of stage fraction on optimum *COP*

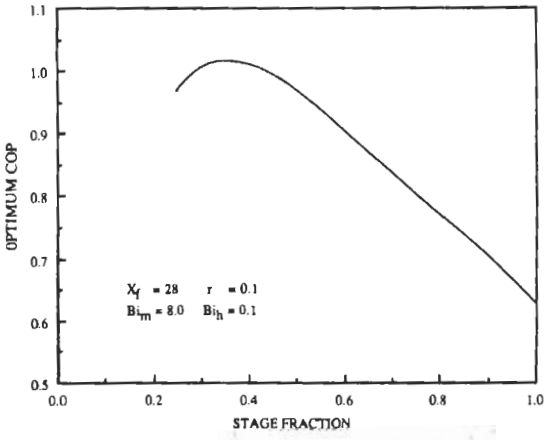

Figure 10. Effect of stage fraction on cooling capacity at the cycle time of optimum *COP*

decreases with increasing SF. The cooling capacity increases continuously with increasing SF because the desiccant is drier with higher SF (more heating) after desorption process, therefore it is capable of adsorbing more moisture which results in higher cooling capacity. At SF=1 (continuous heating); the COP is very low, about 0.63, and the cooling capacity is maximum, about 21. But at SF=0.4, the COP has nearly the maximum value, about 1.0 while the cooling capacity decreases to 17. Consequently, a COP increase by 37% can be expected in this case with a corresponding cooling capacity defect of only 20%.

Effect of Mass Transfer Biot Number

The diffusion of moisture in the desiccant material can be described by gas phase diffusion and surface diffusion. The mass transfer Biot number (Bi_m) which is based only on the gas-phase diffusion resistance is defined as

$$Bi_m = \frac{K_y a_d}{\rho_a D_G} \tag{16}$$

In order to investigate the effect of this parameter, two different cases are considered. One is for D_S=0 and the other is for variable D_S proposed by Sladek et al (18) and is given by

$$D_s = 1.6 \times 10^{-6} \exp(-0.974 \frac{Q}{T}) \tag{17}$$

Figures 11 and 12 show the effect of mass transfer Biot number on the optimum COP and the cooling capacity at the cycle time of optimum COP for these two cases. The results indicate that the optimum COPs for both cases decrease with increasing mass transfer Biot number. The COPs of both cases are very close at the small Bi_m (less than 5). In this region, the surface diffusivity (D_S), which is given by Equation (17), is negligible as compared to D_G. In the region of large Bi_m where the surface diffusion is significant, the COP decreases very slowly with increasing Bi_m when D_S is considered and the COP decreases very rapidly when only the gas-phase diffusion is considered (D_S=0). The cooling capacity curves of Figure 12 have similar trends as the COP curves.

Effect of Overall Mass Transfer NTU

The overall mass transfer NTU can be defined as

$$NTU_{om} = \frac{U_m A}{\dot{m}_p} \tag{18}$$

where the overall mass transfer coefficient (U_m) is given by

$$\frac{1}{U_m} = \frac{1}{K_y} + \frac{a_d}{\rho_a D_G + \rho_d D_s \frac{\partial W_d}{\partial Y_d}} \tag{19}$$

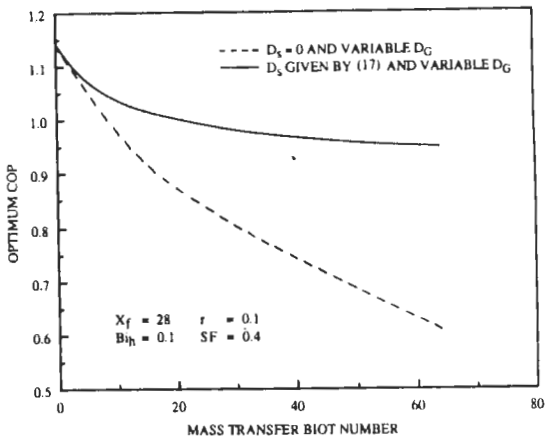

Figure 11. Effect of mass transfer Biot number on optimum *COP*

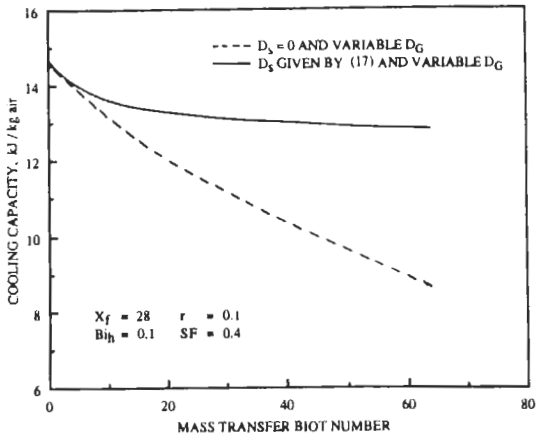

Figure 12. Effect of mass transfer Biot number on cooling capacity at the cycle time of optimum *COP*

Also, the overall mass transfer Biot number can be expressed as

$$Bi_{mo} = \frac{K_y a_d}{\rho_a D_G + \rho_d D_s \frac{\partial W_d}{\partial Y_d}} \tag{20}$$

Therefore the overall mass transfer NTU is related to the overall mass transfer Biot number by

$$NTU_{om} = \frac{NTU_{fm}}{1 + Bi_{mo}} \tag{21}$$

where NTU_{fm} = mass transfer NTU based on film resistance only and is given by

$$NTU_{fm} = \frac{K_y A}{\dot{m}_p} \qquad (22)$$

The overall mass transfer Biot number and the overall mass transfer NTU are calculated using the following parameters:

$$X_f = 2NTU_{fm} = 28$$

$$\frac{\partial W_d}{\partial Y} \cong 3.15$$

$$\frac{K_y a_d}{\rho_a} \cong 1.6848 \times 10^{-4}$$

The results are listed in Table 2 for variable D_S given by Equation (17) and in Table 3 for D_S=0.

Table 2. Relationship between mass transfer Biot number and overall mass transfer NTU for a given value of D_s and variable D_G

Bi_m	D_G	$D_s \frac{\rho_d}{\rho_a} \frac{\partial W_d}{\partial Y_d}$	Bi_{mo}	NTU_{om}
0	∞	0.61×10^{-5}	0.00	14.00
1	0.1685×10^{-3}	0.61×10^{-5}	0.97	7.12
4	0.4212×10^{-4}	0.61×10^{-5}	3.50	3.11
8	0.2106×10^{-4}	0.61×10^{-5}	6.20	1.95
16	0.1053×10^{-4}	0.61×10^{-5}	10.13	1.26
32	0.5265×10^{-5}	0.61×10^{-5}	14.80	0.89
64	0.2633×10^{-5}	0.61×10^{-5}	19.30	0.69

Table 3. Relationship between mass transfer Biot number and overall mass transfer NTU for $D_s = 0$ and variable D_G

Bi_m	D_G	Bi_{mo}	NTU_{om}
0	∞	0.0	14.00
0.5	0.3369×10^{-3}	0.5	9.33
1	0.1685×10^{-3}	1.0	7.00
2	0.8424×10^{-3}	2.0	4.67
4	0.4212×10^{-4}	4.0	2.80
8	0.2106×10^{-4}	8.0	1.56
16	0.1053×10^{-4}	16.0	0.82
32	0.5265×10^{-5}	32.0	0.42
64	0.2633×10^{-5}	64.0	0.22

Figure 13 show the effect of overall mass transfer NTU on the thermal COP as compared to those of Collier (13) where the solid-side resistance is represented by an artificially increased film resistance. As can be seen, the lumped-resistance model used by Collier predicts a faster decrease in COP with decreasing NTU_{om} as compared to the results of present model which properly handles the internal resistances. In Collier's case, a COP decrease of 8% can be expected if the overall mass transfer NTU is reduced from 14 to 7. In the present simulation, the COP decreases by only 2% for the same NTU reduction.

Figure 14 shows the effect of overall mass transfer NTU on the cooling capacity. The cooling capacity decrease with overall mass transfer NTU is slightly less than the COP decrease.

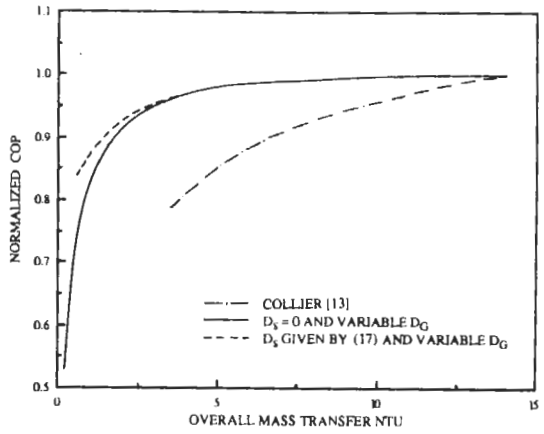

Figure 13. Effect of overall mass transfer *NTU* on *COP* of desiccant cooling system with staged regeneration

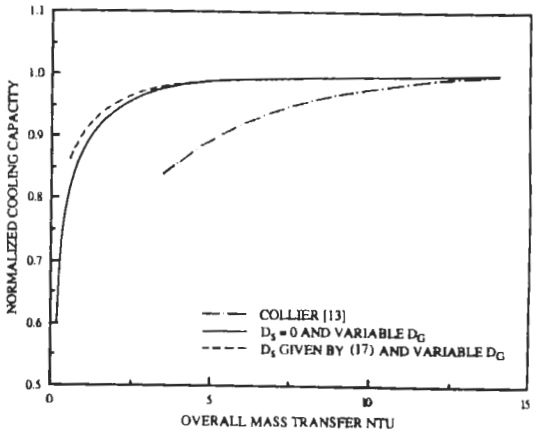

Figure 14. Effect of overall mass transfer *NTU* on cooling capacity of desiccant cooling system with staged regeneration

It can be concluded that the cooling system performance degradation due to solid-side mass transfer resistance is much less than due to increased film resistance that yields the same overall resistance. The reason being that the effect of solid side resistance kicks in gradually as time progresses while the effect of film resistance is immediate.

CONCLUSIONS

A mathematical model, which considers both gas-side and solid-side resistances for heat and mass transports, is used to investigate the performance of an open-cycle desiccant cooling system with staged regeneration. The results show that the cooling system performance can be substantially increased using the staged regeneration concept. Under the same operating conditions, the COP is approximately 1.0 as compared to about 0.6 for the conventional system without staged regeneration.

The results indicate that the optimum cycle time is almost unaffected by the change in stage fraction. Also, the internal mass transfer resistances affect the changes of COP and cooling capacity in the same trend. Finally, there is a minimal effect of the solid-side resistance on the performance of the cooling system.

ACKNOWLEDGMENT

This work is supported in part as a subcontract from the Gas Research Institute through the LaRoche Chemicals Inc.

REFERENCES

1. Pennington, N. A., "Humidity Changer for Air-Conditioning," U. S. Patent No. 2,700,537, January 1955.

2. Dunkle, R. V., "A Method of Solar Air-Conditioning," Mech. and Chem. Eng. Trans., I.E. Australia, 1965, Vol. 1, pp. 73-78.

3. Jurinak, J., "Open-Cycle Solid Desiccant Cooling Component Models and System Simulation," Ph. D. Thesis, University of Wisconsin, Madison, 1982.

4. Nelson, J. S., et al., "Simulation of the Performance of Open-Cycle Desiccant System Using Solar Energy," Solar Energy, 1978, Vol. 21, pp. 273-278.

5. Huskey, B., Sharp, J., Venero, A. and Yen, H., "Advanced Solar/Gas Desiccant Cooling System," GRI-81/0064, Gas Research Institute, Chicago, IL, 1982.

6. Collier, R. K., and Cohen, B. M., "An Analytical Examination of Methods for Improving the Performance of Desiccant Cooling Systems," International Solar Energy Conference, Denver, CO, 1988.

7. Worek, W. M. and Lavan, Z., "Performance of a Cross-Cooled Desiccant Dehumidifier Prototype," ASME Journal of Solar Energy Engineering, 1982, Vol. 104, No. 3, pp. 187-196.

8. Mathiprakasam, B., "Performance Predictions of Silica Gel Desiccant Systems," Ph. D. Thesis, Illinois Institute of Technology, Chicago, 1979.

9. Glav, B. O., "Air Conditioning Apparatus," U.S. Patent No. 3,251,402 , May 1966.

10. Banks, P. J., Close, D. J. and Maclaine-cross, I. L., "Coupled Heat and Mass Transfer in Fluid Flow through Porous Media - An Analogy with Heat Transfer," Journal of Heat Transfer, 1970, Vol. VII, CT3.1, pp. 1-10.

11. Roy, D. and Gidaspow, D., "Nonlinear Coupled Heat and Mass Exchange in a Cross-Flow Regenerator," Chemical Engineering Science, 1974, Vol. 29, pp.2101-2114.

12. Mathiprakasam, B. and Lavan, Z., "Performance Predictions for Adiabatic Desiccant Dehumidifiers Using Linear Solutions," ASME Journal of Solar Energy Engineering, 1980, Vol. 102, pp.73-79.

13. Collier, R. K., "Desiccant Properties and Their Effect on Cooling System Performance," ASHRAE Transactions, 1989, Vol. 95, CH-89-11-1.

14. Bullock, C. E. and Threlkeld, J. L., "Dehumidification of Moist Air by Adiabatic Adsorption," ASHRAE Transactions, 1966, Vol. 72, pp. 301-313.

15. Chi, C. W. and Wasan, D. T., "Fixed Bed Adsorption Drying," AIChE Journal, 1970, Vol. 16, No. 1, pp. 23-31.

16. Mei, V. and Lavan, Z., "Performance of Cross-Cooled Desiccant Dehumidifiers, ' ASME Journal of Solar Energy Engineering, 1983, Vol. 105, No. 3, pp. 300-304.

17. Charoensupaya, D. and Worek, W. M., "Effect of Adsorbent Heat and Mass Transfer Resistances on Performance of an Open-Cycle Adiabatic Desiccant Cooling System," Heat Recovery Systems and CHP, 1988, Vol. 8, No. 6, pp. 537-548.

18. Sladek, K. J., Gilliland, E. R. and Baddour, R. F., "Diffusion on Surfaces. II. Correlation of Diffusivities of Physically and Chemically Adsorbed Species," Ind. Eng. Chem., Fundam., 1974, Vol.13, No. 2, pp. 100-105.